Finite-size-scaling analysis of a simulation of the ^{4}He superfluid transition

E. L. Pollock and Karl J. Runge
Physics Department, Lawrence Livermore National Laboratory, University of California, Livermore, California 94550
(Received 3 February 1992)

Several finite-size scaling techniques are applied to path-integral simulations of the superfluid transition in three-dimensional (3D) ^{4}He at low pressure. The twist free energy shows a linear increase with periodic cell length below the transition temperature, which it predicts as 2.19±0.02 K. (The experimental value is 2.172 K.) Fitting the superfluid fraction to the scaled form $L\rho_s(t,L)/\rho = Q(L^{1/\nu}t)$, $t=(T-T_c)/T_c$, gives $T_c=2.17\pm0.05$ K and the correlation-length exponent $\nu=0.72\pm0.1$ (experimentally 0.67). The universal constant $(\hbar^2\rho/mkT_c)Q(0)=0.50\pm0.02$ found here compares well with the value 0.49±0.01 from recent 3D XY model simulations. Additional analyses that include corrections to scaling are found to yield values for T_c in agreement with the above estimates. A phenomenological renormalization analysis suggests the superfluid density exponent $\upsilon=(1.0-1.3)\nu$, consistent with the Josephson relation.

I. INTRODUCTION

Finite-size scaling is now routinely used to interpret Monte Carlo simulations of phase transitions.[1] The models simulated are usually classical degrees of freedom confined to lattice sites. Here we apply finite-size scaling methods to a path-integral Monte Carlo simulation of the superfluid transition in three-dimensional (3D) ^{4}He.[2] An advantage of this system is that the λ line provides a line of critical points for a range of densities, and so it is not necessary to simultaneously search for a critical density and temperature, as had to be done in the analysis of finite-size data for the liquid-vapor critical point in a classical Lennard-Jones system.[3] A disadvantage is that the necessary path-integral simulations are computationally intensive and statistical accuracy of better than 2% in the superfluid fraction is difficult to achieve. Nonetheless, a transition temperature reliable to within a few hundredths of a degree and critical exponents consistent with experimental values are obtained. A finite-size analysis of simulations of the 2D superfluid transition[4] by fitting to the vortex core radius and formation energy parameters of an XY model, as suggested by Kotsubo and Williams,[5] gave a bulk transition temperature in good agreement with experiment.

A variety of methods for performing finite-size scaling analysis on Monte Carlo data have been suggested. Here we apply a number of them to the superfluid transition in 3D ^{4}He. Perhaps the most intuitive analysis is to examine the twist free energy, defined as the free energy difference caused by changing from periodic to antiperiodic boundary conditions in one direction, as a function of system size. This free energy change will increase with system size in the ordered phase and decrease toward zero exponentially in the disordered phase. In a path-integral calculation it can be easily computed from the winding number distribution as discussed below and provides a clear indication of the transition. As a second method, estimates of the transition temperature and correlation length exponent ν are obtained by requiring the superfluid fractions for the various system sizes and temperatures to collapse onto a single scaled form. Thirdly, we employ a technique that incorporates the expected form of corrections to scaling to provide another estimate of the transition temperature. Lastly, the phenomenological renormalization method suggested by Barber and Selke[6] is used to obtain a value for the superfluid fraction exponent υ, which is found to agree with the Josephson relation $\upsilon=\nu$.

II. ANALYSIS

Path-integral techniques and their use in calculating superfluid densities are discussed in Ref. 2. The data there for systems of $N=64$ ^{4}He particles in a periodic cell has been augmented with additional simulations primarily for smaller periodic systems ($N=32$, 16, and 8). The choice of interparticle potential specifying the Hamiltonian is described in Ref. 7. For reference all the data used in this paper are given in Table I.

A. Twist free energy

The twist free energy, defined as the free energy change, produced by switching from periodic to antiperiodic boundary conditions along one direction,[8] would be intuitively expected to scale very differently with system size in the ordered and disordered phases. For a system with a one-component order parameter, such as the Ising model, this free energy change in the ordered phase well below the transition temperature is proportional to the number of spins reversed in imposing the antiperiodic boundary conditions. In 3D this is given by the area L^2, where L is the cell length, so that $\Delta F \propto L^2$. For a system with a two-component order parameter, such a superfluid ^{4}He or the XY model, spin wave theory, valid at low temperature, gives

$$\Delta F = \tfrac{1}{2}\int \Upsilon(\nabla\theta)^2 d^3r \qquad (1)$$

as the free energy cost in imposing a phase variation $\theta(r)$ on the system. For antiperiodic boundary conditions along one direction $\nabla\theta=\pi/L$ and

$$\Delta F=\tfrac{1}{2}\Upsilon(\pi/L)^2L^3\propto L \ . \tag{2}$$

The constant helicity modulus Υ is proportional to the superfluid density for the case of ^{4}He.[9] In the high temperature phase ΔF is expected to decrease exponentially with the correlation length ξ, $\Delta F\sim e^{-L/\xi}$.

In a periodic system the density matrix is periodic. This arises naturally in a path-integral computation by allowing the path for an N-particle system originating at $\{\mathbf{r}_1,\mathbf{r}_2,\ldots,\mathbf{r}_N\}$ to end at $\{\mathbf{r}_1'+\mathbf{L}_1,\mathbf{r}_2'+\mathbf{L}_2,\ldots,\mathbf{r}_N'+\mathbf{L}_N\}$ where $\{\mathbf{L}_1,\mathbf{L}_2,\ldots,\mathbf{L}_N\}$ are any set of lattice vectors including the most likely value $\mathbf{L}_1=\mathbf{L}_2=\cdots=\mathbf{L}_N=0$. This brings in the winding number[2]

$$\mathbf{W}=\frac{1}{L}\sum_{j=1}^{N}(\mathbf{r}_j-\mathbf{r}_j'-\mathbf{L}_j) \tag{3}$$

which is defined for every path configuration. Viewing the periodic space as a toroid, $\mathbf{W}$ describes the number of times the paths wind around the toroid. As shown in Ref. 2, the superfluid density is given by $\rho_s/\rho=(mkT/3\hbar^2N)\langle\mathbf{W}^2\rangle L^2$.

To switch from periodic to antiperiodic boundary conditions (in say the z direction) it is only necessary to correct the density matrix by reweighting each path configuration with $e^{iW_zL\pi/L}=e^{iW_z\pi}$ so that the paths ending $\pm L$, $\pm 3L$, etc., from their origins pick up a minus sign. Since the partition function $\mathcal{Z}$, is given by the integral over the diagonal density matrix a little algebra gives

$$e^{-\beta\Delta F}=\frac{\mathcal{Z}_{AP}}{\mathcal{Z}_P}=\langle e^{iW_z\pi}\rangle \tag{4}$$

or

$$\Delta F=-kT\ln\langle e^{iW_z\pi}\rangle \ , \tag{5}$$

where $\langle\cdots\rangle$ denotes averaging over all configurations generated in the periodic case. The winding number distributions, $P(W_z)$, necessary to compute this average are given in Table I.

ΔF as a function of cell length L is plotted in Fig. 1 for several temperatures near the transition temperature and

TABLE I. Superfluid fractions and winding number probabilities. The 4 blocks of data (from the top) are for $N=64$, $N=32$, $N=16$, and $N=8$ particle periodic systems. The density is 0.02197 particles/Å^3 (or a molar volume of 27.41 cm^3) except for the $N=64$, $T=1.6$, 1.818, and 2.0 cases for which $\rho=0.021\,83$, $0.021\,86$, and $0.021\,91$ particles/Å^3, respectively.

T	ρ_s/ρ	$P(W=0)$	$P(W=\pm1)$	$P(W=\pm2)$	$P(W=\pm3)$	$P(W=\pm4)$	$P(W=\pm5)$
1.60	0.865(32)	0.2719	0.2218	0.1058	0.0306	0.0048	0.0008
1.818	0.657(22)	0.3515	0.2326	0.0769	0.0130	0.0017	
2.0	0.471(16)	0.4569	0.2210	0.0457	0.0048		
2.105	0.411(17)	0.5268	0.1991	0.0337	0.0035	0.0003	
2.222	0.218(12)	0.6944	0.1420	0.0105	0.0003		
2.35	0.159(12)	0.7849	0.1015	0.0055	0.0006		
2.50	0.090(2)	0.8788	0.0580	0.0027			
1.6	0.838(17)	0.3282	0.2278	0.0859	0.0197	0.0023	0.0002
1.8182	0.693(11)	0.3925	0.2314	0.0622	0.0097	0.0005	
1.905	0.655(15)	0.4283	0.2228	0.0551	0.0074	0.0005	
2.0	0.557(19)	0.4793	0.2140	0.0420	0.0042	0.0001	
2.1056	0.471(20)	0.5613	0.1852	0.0312	0.0028	0.0001	
2.2222	0.314(11)	0.6766	0.1458	0.0150	0.0008		
2.353	0.225(8)	0.7611	0.1116	0.0076	0.0003		
2.5	0.145(8)	0.8433	0.0753	0.0003	0.0001		
1.6	0.862(15)						
1.739	0.798(11)	0.4061	0.2287	0.0596	0.0080	0.0006	
1.8182	0.752(11)	0.4402	0.2210	0.0517	0.0068	0.0004	
1.905	0.700(14)	0.4739	0.2130	0.0450	0.0047	0.0003	
2.0	0.621(9)	0.5182	0.2026	0.0352	0.0029	0.0001	
2.105	0.544(12)	0.5781	0.1818	0.0269	0.0022	0.0001	
2.2222	0.421(11)	0.6604	0.1521	0.0168	0.0009		
2.353	0.370(9)	0.7078	0.1329	0.0126	0.0006		
2.5	0.310(9)						
1.818	0.839(10)	0.4609	0.2211	0.0441	0.0042	0.0002	
1.905	0.797(8)						
2.105	0.711(10)	0.5551	0.1927	0.279	0.0018	0.0001	
2.222	0.662(9)	0.5939	0.1788	0.0229	0.0014		
2.353	0.572(9)	0.6477	0.1594	0.0158	0.0009		
2.5	0.521(8)	0.6872	0.1434	0.0124	0.0005		

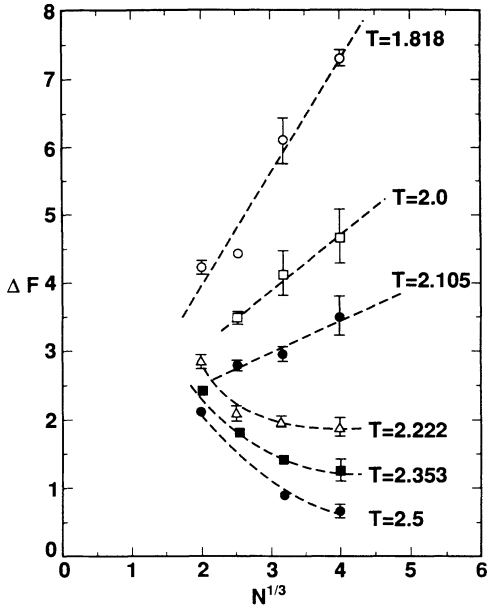

FIG. 1. Free energy difference $\Delta F = F_{AP} - F_P$ (in K) between antiperiodic and periodic boundary conditions for the indicated temperatures as a function of system size. The straight lines at low T are linear fits. The curves for the three high T points are to guide the eye.

clearly shows the change from a linear increase at low temperature to a decrease above the transition temperature T_c. An estimate of T_c based on extrapolating the slopes of the curves to zero gives $T_c = 2.19 \pm 0.02$.

B. Scaling function fit

According to the basic hypothesis of finite-size scaling,[10] near the critical point T_c the intensive properties of a system depend on the system size L only through the ratio of L to the bulk correlation length $\xi(T)$. This implies that if the bulk superfluid fraction behaves like $\rho_s(t)/\rho \sim t^v$, $t \equiv (T - T_c)/T_c$, near $t = 0$ then its finite-size behavior obeys the scaled form

$$\rho_s(t,L)/\rho \sim L^{-v/\nu} Q(L^{1/\nu} t) , \tag{6}$$

where ν is the correlation length exponent [$\xi(t) \sim t^{-\nu}$]. The function Q is unknown but must be analytic for finite argument since this corresponds to a finite-size system.

We have made another estimate of T_c and ν by trying a linear form for Q and varying T_c and ν to minimize the deviation of the data from this line. It was assumed that $v/\nu = 1$ since this is indicated by experiment,[11] renormalization-group calculation,[12] and the Josephson hyperscaling relation $v = (d-2)\nu$. The assumption $v/\nu = 1$ will be shown later to be compatible with our data.

Figure 2 shows the scaled data and the resulting linear fit. (The two points farthest away from the transition region were not used in the fit.) The best fit parameters were $T_c = 2.17 \pm 0.05$ and $\nu = 0.72 \pm 0.1$. The value of T_c was more stable to variations in this procedure than was the value of ν. For example, fitting a quadratic to the data shifted T_c to 2.19 and ν to 0.57.

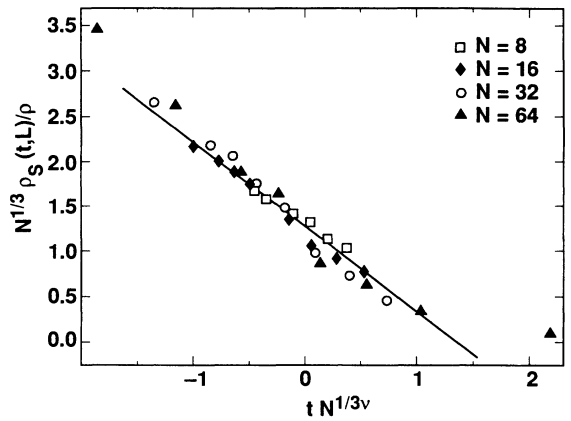

FIG. 2. Scaled superfluid fraction $N^{1/3}\rho_s(T,L)/\rho$ vs $tN^{1/3\nu}$ for periodic systems of 8, 16, 32, and 64 particles. The best linear fit (dashed line) was for $T_c = 2.17 \pm 0.05$ and $\nu = 0.72 \pm 0.1$.

C. Corrections to scaling

It follows from Eq. (6) that at the critical point the superfluid density goes to zero as $L^{-v/\nu}$ and that the functions $L^{v/\nu}\rho_s(T,L)/\rho$ (given by different values of L) all cross at $T = T_c$. Assuming $v = \nu$, this quantity is plotted in Fig. 3. One can see that the intersections occur near the experimental critical point $T_c = 2.17$, however, for the smaller L values there is a systematic deviation toward smaller T. This shift is due to corrections to scaling which we take into account as follows.

From finite-size scaling in the presence of a nonvanishing irrelevant scaling field ζ one expects that[13]

$$L\rho_s(t,L)/\rho = Q_2(tL^{1/\nu}, \zeta L^{-\Delta/\nu}) , \tag{7}$$

where the correction to scaling exponent Δ has been calculated as 0.521 ± 0.006.[12] $Q_2(x,y)$ must be a regular function of its arguments, and, so, may expand near

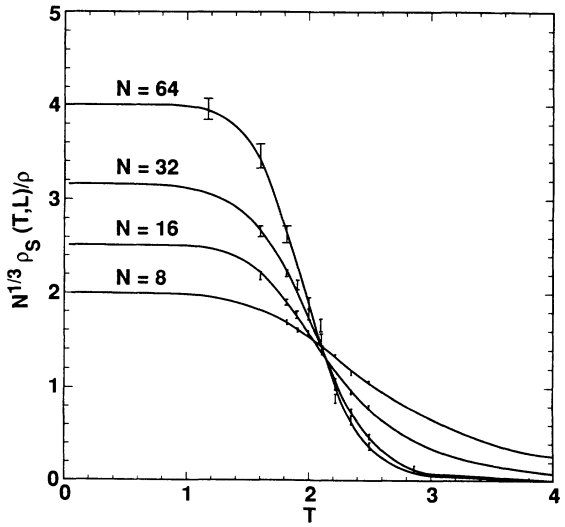

FIG. 3. Scaled superfluid fraction $N^{1/3}\rho_s(T,L)/\rho$ vs T for periodic systems of 8, 16, 32, and 64 particles. The solid lines are to guide the eye.

$t=0$

$$L\rho_s(t,L)/\rho \approx Q_2^{(0)}(1+atL^{1/\nu}+bL^{-\Delta/\nu}+\cdots) . \quad (8)$$

If we denote by t_{12} the intersection point of system sizes L_1 and L_2, then Eq. (8) predicts

$$t_{12} \propto (L_1^{-\Delta/\nu}-L_2^{-\Delta/\nu})/(L_1^{1/\nu}-L_2^{1/\nu}) \equiv \delta_{12} \quad (9)$$

or that $T_{12}=T_c+c\delta_{12}+\cdots$. This implies that T_{ij} plotted versus δ_{ij} for all pairs should yield a straight line with intercept equal to the infinite system transition temperature T_c. For each L, the data in Table I were fit to a 4-parameter function of T (displayed in Fig. 3). The average intersection point T_{ij} and its associated error were estimated via the synthetic data method.[14] The T_{ij} obtained are consistent with a linear dependence on δ_{ij}. A final least-squares fit yields $T_c=2.21\pm0.03K$. The value was found to be fairly insensitive to the choice of the correction to scaling exponent $0.25<\Delta<0.75$.

For large size systems we estimate the value at the crossing point in Fig. 4 as $Q(0)=4.1\pm0.2$ Å (after converting the $N^{1/3}$ to L). The universal constant $(\hbar^2\rho/mkT_c)Q(0)=0.50\pm0.02$ should have the same value for the 3D XY model which is in the same universality class. Recent simulations of that model[15] give 0.49 ± 0.01. That the two systems are in the same universality class has long been accepted but it is gratifying to see this agreement between simulations of "real" helium and a classical spin system.

Another commonly used estimate of T_c examines the location of the specific heat maximum, $T_{\max}(L)$. Finite-size scaling indicates[10] that the correction is of the form $T_{\max}(L)\approx T_c+a/L^{1/\nu}$. Although the path-integral Monte Carlo data for the specific heat is rather noisy (having come from differentiating a fit to the total energy), the $N=16,32,64 T_{\max}(L)$ are consistent with the predicted form and yield $T_c=2.23\pm0.07$. Thus, the finite-size corrected estimates for the transition point are slightly larger but consistent with that obtained from the twist free energy and scaling function methods and also with the experimental value.

D. Phenomenological renormalization

A final analysis of the Monte Carlo data in the critical region was performed using phenomenological renormalization,[6] in which one defines the ratio

$$R_{L_1,L_2}(T)=\rho_s(T,L_1)/\rho_s(T,L_2) . \quad (10)$$

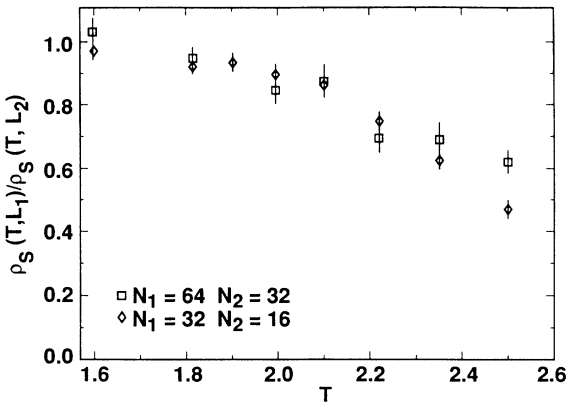

FIG. 4. Ratio of $\rho_3(T,L_1)/\rho_s(T/L_2)$ vs T for $N_1=64$, $N_2=32$ and $N_1=32$, $N_2=16$. The two curves should cross at $T=T_c\approx2.17$ at a value of $0.794^{\upsilon/\nu}$.

In the critical region

$$R_{L_1,L_2}(T)=\left[\frac{L_1}{L_2}\right]^{-\upsilon/\nu}\frac{Q(L_1^{1/\nu}t)}{Q(L_2^{1/\nu}t)} \quad (11)$$

from Eq. (6) and in particular

$$R_{L_1,L_2}(T_c)=\left[\frac{L_1}{L_2}\right]^{-\upsilon/\nu} . \quad (12)$$

Figure 4 shows $R_{L_1,L_2}(T)$ for two cases: $N_1=64$, $N_2=32$ and $N_1=32$, $N_2=16$. Since $L_1/L_2=2^{1/3}$ for both cases, these curves should cross at $(T_c,2^{-\upsilon/3\nu})=(T_c,0.794^{\upsilon/\nu})$. The statistical uncertainty in the data is too large to accurately determine T_c from the crossing of these two curves however, assuming $T_c\approx2.17$ then from the figure $R_{L_1,L_2}(T_c)\approx0.74$–$0.80$ or $\upsilon/\nu\approx1.0$ to 1.3.

In conclusion the finite-size scaling analysis described above for a path-integral simulation of the superfluid transition in 3D ^{4}He yields a transition temperature, critical exponents ν and υ, and the universal constant $(\hbar^2\rho/mkT_c)Q(0)$ in good agreement with experiment and calculations on other models in the same universality class.

ACKNOWLEDGMENTS

The authors thanks M. P. Nightingale for his help. The work performed at Lawrence Livermore National Laboratory was supported under the U.S. Dept. of Energy Contract No. W-4705-ENG-48.

[1] *Finite Size Scaling and Numerical Simulation of Statistical Systems*, edited by V. Privman (World Scientific, Singapore, 1990).
[2] E. L. Pollock and D. M. Ceperley, Phys. Rev. B **36**, 8343 (1987).
[3] M. Rovere, D. W. Heermann, and K. Binder, J. Phys.: Condens. Matter **2**, 7009 (1990).
[4] D. M. Ceperley and E. L. Pollock, Phys. Rev. B **39**, 2084 (1989).
[5] V. Kotsubo and G. A. Williams, Phys. Rev. B **33**, 6106 (1986).
[6] Michael N. Barber and Walter Selke, J. Phys. A **15**, L15 (1982).
[7] R. A. Aziz, V. P. S. Nain, J. S. Carley, L. W Taylor, and G. T. McConville, J. Chem. Phys. **70**, 4330 (1979).
[8] *Finite Size Scaling and Numerical Stimulation of Statistical Systems* (Ref. 1), p. 49.
[9] M. E. Fisher, M. N. Barber, and D. Jasnow, Phys. Rev. A **8**,

1111 (1973).

[10]M. N. Barber, in *Phase Transitions and Critical Phenomena,* edited by C. Domb and J. L. Lebowitz (Academic, New York, 1983), Vol. 8, p. 145 (see particularly pp. 158–160).

[11]Dennis S. Greywall and Geunter Ahlers, Phys. Rev. A **7**, 2145 (1973).

[12]J. C. Le Guillou and J. Zinn-Justin, Phys. Rev. Lett. **39**, 95 (1977).

[13]M. N. Barber, in *Phase Transitions and Critical Phenomena* (Ref. 10), pp. 170 and 171.

[14]W. H. Press, B. P. Flannery, S. A. Teukolsky, and W. T. Vetterling, *Numerical Recipes* (Cambridge University Press, Cambridge, England, 1986), pp. 529–532.

[15]Ying-Hong Li and S. Teitel, Phys. Rev. B **40**, 9122 (1989); W. Janke, Phys. Lett. A **148**, 306 (1990); Min-Chul Cha, Matthew, P. A. Fisher, S. M. Girvin, Mats Wallin, and A. Peter Young, Phys. Rev. B **44**, 6883 (1991); in particular, see Fig. 5 of this paper.